physica status solidi rrl

www.pss-rapid.com

Benchmarking Electrolyte-Gated Monolayer MoS_2 Field-Effect Transistors in Aqueous Environments

*Steffen Rühl, Max Heyl, Fabian Gärisch, Sylke Blumstengel, Giovanni Ligorio, and Emil J. W. List-Kratochvil**

Most electrical sensor and biosensor elements require reliable transducing elements to convert small potential changes into easy to read out current signals. Offering inherent signal magnification and being operable in many relevant environments field-effect transistors (FETs) are the element of choice in many cases. In particular, using electrolyte gating, numerous sensors and biosensors have been realized in aqueous environments. Over the past years, electrolyte-gated FETs have been fabricated using a variety of semiconducting materials, including graphene, ZnO, as well as conjugated molecules and polymers. Above all, using conducting polymers top-performing devices have been achieved. Herein, an approach to use a transition metal dichalcogenide (TMDC)-based monolayer device as a transducing element is presented. Using MoS_2 monolayers, it is shown that such electrolyte-gated devices may be regarded as very promising transducing elements for sensor and biosensor applications, enabled by their high sensitivity for environmental changes and the possibility of using the naturally occurring sulfur vacancies as grafting points of biorecognition layers. Furthermore, the behavior of such a device under prolonged operation in a dilute biologically relevant electrolyte such as phosphate buffered saline solution (PBS) is reported.

1. Introduction

Using electrolyte gating to control the electronic properties of various classes of semiconductors via the formation of an electric double layer (EDL) at the semiconductor/electrolyte interface or via a Faradaic charge transfer processes across this interface has helped to unravel novel material properties[1] and also found its way into many practical device applications.[2–4] In particular, field-effect transistor (FET)-based applications benefit from electrolyte gating. Because the high capacitance values (1–100 $\mu F\,cm^{-2}$) achieved,[5] low voltage operation (<1 V) becomes possible, which paves the way for FETs as effective transducing elements to convert gate potential variations ΔV_G into source–drain currents ΔI_D in sensors[6,7] and biosensors[5,8–11] in aqueous environments. In such applications, the figure of merit that determines the effectiveness of this conversion is the transconductance (g_m), which is defined as $g_m = \Delta I_D/\Delta V_G$. Here, conducting polymer-based organic electrochemical transistor (OECT) is currently the top performer with a typical g_m of 2.7 mS followed by ZnO and graphene-based devices achieving a g_m of 1.4 and 1.8 mS, respectively.[10]

Inspired by the high-performance values achieved with graphene-based devices,[12,13] 2D semiconductors with their topography-related high sensitivity to the changes at their interfaces seem to constitute the ideal candidates for electrolyte-gated FETs (EGFETs).

One very promising material class of atomically thin semiconductors is the transition metal dichalcogenides (TMDCs). This material class crystalizes in a layered sandwich structure with strong covalent bonds within the MX_2 (M = transitions metal; X = S, Se, Te) layers but comparatively weak interlayer interactions, allowing to cleave off single layers of the bulk crystal. Devices made from monolayers could be described as interface-only devices and applications of TMDCs as gas sensors have already been shown.[14] To be able to use TMDCs in high-performance FET applications, the main challenge to overcome is the defect control of these monolayers.[15] The two main types of defects are grain boundaries and metal or chalcogenide vacancies. Both degrade the electrical performance of the material, yet the vacancies also open up an additional path to covalently functionalize the monolayers, which can be advantageous in sensor applications.[16–20] Recently, the operation of a MoS_2-based FET device utilizing deionized (DI) water has been shown; however, utilizing MoS_2 multilayers.[21,22] These results constitute a promising starting point for benchmarking FETs in

S. Rühl, M. Heyl, F. Gärisch, Dr. S. Blumstengel, Dr. G. Ligorio, Prof. E. J. W. List-Kratochvil
Department of Chemistry
Department of Physics & IRIS Adlershof
Humboldt-Universität zu Berlin
Zum Großen Windkanal 2, Berlin 12489, Germany
E-mail: emil.list-kratochvil@hu-berlin.de

Prof. E. J. W. List-Kratochvil
Helmholtz-Zentrum für Materialien und Energie GmbH
Hahn-Meitner-Platz 1, Berlin D-14109, Germany

The ORCID identification number(s) for the author(s) of this article can be found under https://doi.org/10.1002/pssr.202100147.

DOI: 10.1002/pssr.202100147

biosensor-relevant electrolytes. By fabricating FETs based on MoS_2 monolayers, using aqueous liquids with the required ionic strength and choosing gate electrodes with advantageous properties we will show that one can push the performance of MoS_2 EGFETs to record heights. In addition to basic device characterization, we also perform long-term stability tests and find that MoS_2 EGFETs may be regarded as very promising transducing elements for sensor and biosensor applications.

2. Results and Discussion

Figure 1a,b shows a schematic of the bottom contact EGFETs with typical gate electrodes to bias the transistors in an aqueous environment with a polarizable Pt and a nonpolarizable Ag/AgCl electrode, respectively. Pt is an example of a polarizable electrode, meaning that charge separation occurs at the electrode/electrolyte interface and only little to no current passes which results in the electrode acting as a capacitor, also represented in the equivalent circuit below Figure 1a. In contrast to that the Ag/AgCl electrode shown in Figure 1b is an example for a nonpolarizable electrode, meaning that no EDL is formed at the electrode/electrolyte interface as described in detail in the literature.[23] While using a polarizable electrode, the EDL formed at the semiconductor/electrolyte is typically limited by its surface capacitance. This can be overcome by using a nonpolarizable electrode such as an Ag/AgCl electrode,[5] where the maximum possible EDL capacitance and therefore gating effect can act polarizing on the semiconductor. Figure 1c shows an optical image of an EGFET using an MoS_2 monolayer with a 30 µm long and 1 mm wide channel with bottom contact source–drain electrodes. For a description of the exfoliation and transfer process, see previous studies.[24,25] The outline of the monolayer is accentuated by a dotted red line to highlight the faint contrast between the region covered by monolayer and the bare substrate/electrode. To avoid hydrogen evolution reactions, which may happen at sulfur edge sites in MoS_2,[26] all relevant measurements have been done within a 500 mV potential window. Outside this window, a sudden increase in gate currents can be seen in Figure S1 and S4, Supporting Information, which points toward catalytic activity.

To demonstrate the importance of choosing the proper gate electrode, the device was measured with two different electrodes. To work in a biosensor-relevant environment, PBS (PBS × 10) was chosen as the electrolyte, which was diluted to a NaCl concentration of 10^{-2} M. **Figure 2**a shows the output characteristic of a device measured by using the Pt wire as gate electrode (the architecture is shown in Figure 1a). This device already shows very promising output characteristics when compared with the state of the art,[21,22] showing transport across the channel for gate voltages (V_{GS}) $V_{GS} \geq 300$ mV and reaching saturation drain currents (I_D) of about 2.5 µA for $V_{GS} = 500$ mV. The device shows a second rise in I_D for larger drain source voltages (V_{DS}). The corresponding gate currents for output and transfer characteristics shown in Figure 2a,b utilizing a Pt gate are shown in S3 and when comparing them to Figure S1, Supporting Information, the influence of the different working principles of the electrodes on the gate current can be seen. The device performance can be significantly improved by exchanging the Pt gate electrode to an Ag/AgCl electrode (see Figure 1b). Figure 2c shows the output characteristic using the Ag/AgCl gate with an increase in the saturation current to about 470 µA. This corresponds to almost a 200-fold increase compared with the device using the Pt electrode. When compared, the shape of the output characteristics (Figure 2a,c) also slightly changes as a function of the used electrode. The Pt electrode, when compared with the Ag/AgCl electrode reaches saturation for smaller V_{DS} (<150 mV), shows linear current increase for a smaller V_{DS} range and the pinch off happens over a smaller region. This is an effect of the shifting threshold voltages of different gate electrodes. This shift is as large as the electrochemical potentials of the electrodes are shifted with respect to each other. The transfer measurements for a device with an Ag/AgCl electrode are shown in Figure 2d. This device reaches peak currents of almost 1 mA in saturation, a mobility μ of 26 $cm^2\ V^{-1}\ s^{-1}$, a subthreshold swing

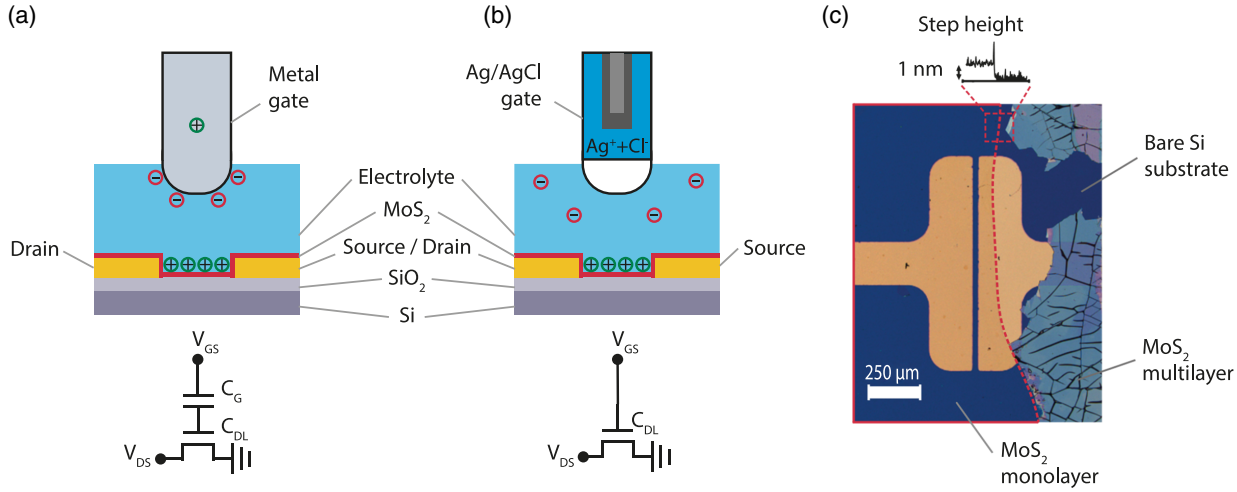

Figure 1. a,b) Schematics of an MoS_2-based EGFET utilizing a polarizable electrode such as Pt (a) and a nonpolarizable electrode (b) as a gate, including the equivalent circuit diagram below. c) Optical microscopy image of an MoS_2-based EGFET. Dotted red line marks the monolayer edge. Inset monolayer step height from atomic force microscopy measurements.

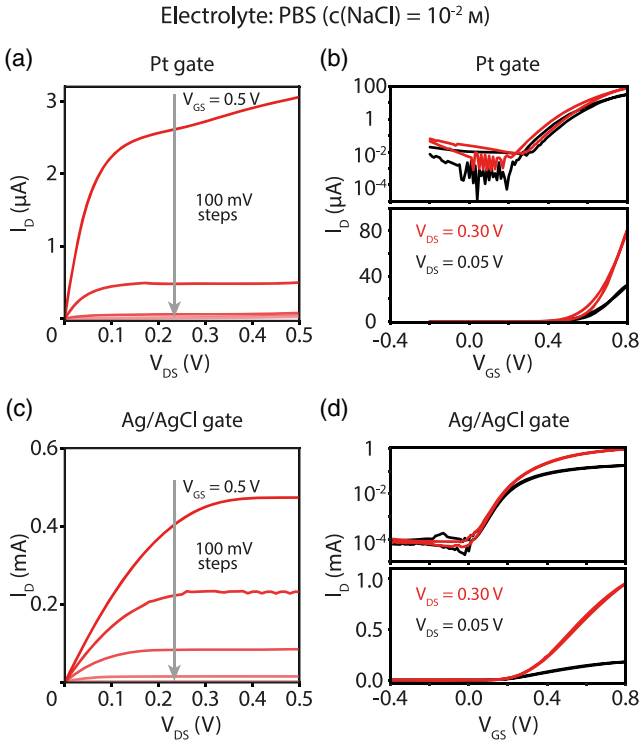

Figure 2. a,c) Monolayer MoS_2EGFET output characteristic using Pt (a) and Ag/AgCl (c) electrodes (3 M inner KCl filling) as a gate in dilute PBS (c(NaCl) = 10^{-2} M). b,d) Corresponding transfer characteristic for the Pt and Ag/AgCl gate, respectively, on a semilogarithmic (top) and linear (bottom) scale.

(SS) of 70 mV dec^{-1} and a threshold voltage V_{Th} of 110 mV. For the linear regime, these values are $\mu = 34\ cm^2\ V^{-1}\ s^{-1}$, SS = 78 mV dec^{-1}, and $V_{Th} = 190$ mV. A constant capacitance of 5.2 μF cm^{-2} was assumed for mobility calculations which was measured via impedance spectroscopy. For the on/off ratio, we find 10^4, which is not as good as values found in the literature.[21] This decrease is attributed to an increase in the off-state current caused by the ionic strength of the electrolyte. In S5 and S6, we show the corresponding device characteristics using DI water with Pt and an Ag/AgCl electrode. The reproducibility is addressed in Table S1, Supporting Information, where an average over 17 devices and the resulting standard deviation of the figures of merit is given. Essentially all device parameters are superior when using PBS as compared with DI water due to the reduced ionic strength of the latter. When operated at negative V_{DS}, I_D does not show a saturating behavior which is accompanied by rising gate currents, an indication for faradaic currents being passed, meaning that there are electrochemical reactions taking place as shown in Figure S1 and S4, Supporting Information. To extract the figure of merit for FETs sensor applications, the transconductance g_m is calculated for the linear and saturation region depending on the applied gate bias (see S2). For the linear region, we find a peak of g_m at $V_{DS} = 50$ mV and $V_{GS} = 360$ mV with $g_m = 0.35$ mS, while in saturation for $V_D = 400$ mV and $V_G = 530$ mV, a top value of $g_m = 1.98$ mS is found. To put these results into perspective, we compared the performance of our device to a literature study on OECTs

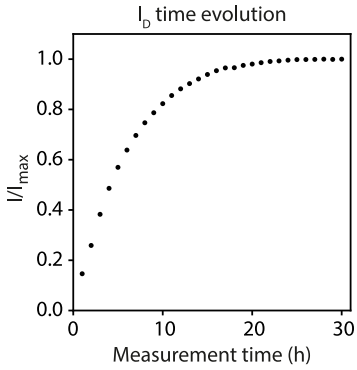

Figure 3. Thirty cycles of 1 h-long measurements have been done consecutively. Electrolyte was changed after the first 15 measurements cycles. Relative current measured after 1 h plotted versus the measurement cycle. Measurements done in dilute PBS ([NaCl] = 10^{-2} M) with $V_{DS} = 50$ mV and $V_{GS} = 400$ mV.

by Khodagholy et al.[10] When compared with the typical performance of a poly(3,4-ethylenedioxythiophene):polystyrene sulfonate (PEDOT:PSS)-based OECT with $g_m = 2.7$ mS, the MoS_2 monolayer device shows comparable top performance. When further putting the transconductance in relation to V_{DS}, our devices outperform the literature example with 7 mS V^{-1} compared with 6.7 mS V^{-1}, although it has to be mentioned that this advantage in performance stems from the device architecture and when the transconductance is put into relation to the channel width (1000 vs 10 μm), the MoS_2-based devices still fall behind the OECTs. The conductivity values reached are 90 S m^{-1} for MoS_2 and 270 S m^{-1} for a typical PEDOT:PSS OECT. OECTs experience what is called a 3D capacitance as ions can migrate into the active layer.[23] For an OECT with a 130 nm-thick PEDOT:PSS layer, the equivalent 2D capacitance would be in the range of 500 μF cm^{-1}, while the presented Ag/AgCl device experiences an capacitance reduced by about two orders of magnitude.[8] This highlights that MoS_2 is performing above its 2D dimensionality and just a single layer exhibits performance almost on-par with the 3D polymeric competitors while still providing the surface-only character-enhancing susceptibility to interfacial sensing events.

To test the device for stability in **Figure 3**, we show the constant operation of the device in 30 consecutive 1 h-long constant measurement cycles. The last data points from the experiments were extracted and plotted versus the measurement time to show the behavior under constant bias stress. We see a steady increase in current until run 17, after which a steady state starts to develop which has fully developed after run 25 and lasting for the next 5 h of measurements after which the experiment was stopped. This behavior shows that the device needs some conditioning before it has reached its peak performance and a constant current.

The exact reason for the necessary conditioning, which was observed in all devices, is not fully understood and is subject to further investigation. One way to avoid the conditioning might be found in modifying the contacts with a thin an insulating polymer layer to avoid electrochemical reactions at the contacts as shown to help for similar devices.[21,24] This would also avoid

a modulation of the contact resistance at the source and drain electrodes has it has been shown in the literature.[27,28] Alternatively we are testing other members from the TMDC material family such as WSe_2 which are known for a more balanced transport and a lower defect density.[29,30]

3. Conclusion

We were able to successfully show the reliable operation of an MoS_2 monolayer-based EGFET in a biologically relevant liquid, showing decent mobility, very low SS, and an exceptional transconductance of ≈2 mS. Although the device does show an increasing current under constant bias at first, after some conditioning of the device the current reaches a saturation level during prolonged operation. The performance may be further improved by modifying the interface to the dielectric substrate to avoid the possibilities of polaron scattering and the introduction of trap states through the oxide interface, as well as by eliminating sulfur and molybdenum vacancies and grain boundaries in the active MoS_2 layer as both are known to degrade electrical performance. Yet given the high transconductance, this MoS_2-based device is an ideal candidate for biosensing, as monolayer materials with their "no-bulk-only-surface" character come with an inherent sensitivity to interfacial changes. Furthermore, the sulfur vacancies may lend themselves as anchoring points for molecular fine-tuning of biorecognition layers.

4. Experimental Section

MoS_2 Exfoliation and Transfer: For the MoS_2 exfoliation, ultraflat template-stripped Au was used as exfoliation membrane. A MoS_2 crystal (2D semiconductors, synthetic MoS_2 crystal) is cleaved with the help of Kapton tape and the freshly exposed MoS_2 surface is pressed onto the ultraflat gold membrane. After heating at 200 °C for 1 min, the MoS_2 carrying Kapton tape can be removed, leaving monolayers on gold behind. For a detailed description of the process and a full MoS_2 characterization, see Heyl et al.[24] For the transfer, polystyrene (PS, Sigma-Aldrich, average $M_w \approx 280\,000$) in toluene (Roth, ROTISOLV HPLC) (80 mg mL^{-1}) was spin-coated onto the exfoliated gold substrates (3500 rpm, 60 s), annealed for 10 min at 80 °C. Finally, the PS/MoS_2/Au membrane was etched in KI/I_2 solution (Sigma-Aldrich, "Au etchant, standard") to remove the Au layer. The final PS/MoS_2 was repeatedly washed in DI water to remove any residual etchant solution and transferred on the final substrate.

FET Preparation: Silicon substrates (1.5 × 2 cm) were ultrasonicated in Hellmanex II and IPA (Roth, ROTISOLV HPLC) and treated in an oxygen plasma for 5 min. FET drain and source electrodes were fabricated by depositing 5 nm of chromium (0.5 Å s^{-1}) and 55 nm of gold (≈1 Å s^{-1}) deposited at a base pressure of 10^{-7} mbar. After transfer of the MoS_2 carrying PS membranes samples were dried, annealed at 150 °C (30 min), and the PS was removed by the help of hot toluene.

Electrical Characterizations: All electrical FET characterization was done with a Keithley 4200A-SCS Parameter Analyzer using an Ossila OFET test board using a polydimethylsiloxane (PDMS) pool to hold the diluted electrolyte (Alfa Aesar, PBS 10×, pH 7.4), which was equipped with a glass cover with a small hole to account for the electrode.

Supporting Information

Supporting Information is available from the Wiley Online Library or from the author.

Acknowledgements

The authors would like to acknowledge Paul Zybarth and Bodo Kranz for their continuous support in the lab. The authors gratefully acknowledge financial support by the Deutsche Forschungsgemeinschaft (Projektnummer 182087777 – SFB 951). This work was conducted in the framework of the Joint Lab GEN_FAB and was supported by the HySPRINT Innovation Lab at Helmholtz-Zentrum Berlin.

Open access funding enabled and organized by Projekt DEAL.

Conflict of Interest

The authors declare no conflict of interest.

Data Availability Statement

The data that support the findings of this study are available from the corresponding author upon reasonable request.

Keywords

electrolyte gated transistors, MoS_2, sensor applications, transition metal dichalcogenides, water

Received: March 15, 2021
Revised: May 31, 2021
Published online: July 6, 2021

[1] S. Z. Bisri, S. Shimizu, M. Nakano, Y. Iwasa, *Adv. Mater.* **2017**, *29*, 1607054.
[2] K. H. Lee, M. S. Kang, S. Zhang, Y. Gu, T. P. Lodge, C. D. Frisbie, *Adv. Mater.* **2012**, *24*, 4457.
[3] K. Schmoltner, J. Kofler, A. Klug, E. J. W. List-Kratochvil, *Adv. Mater.* **2013**, *25*, 6895.
[4] J. Rivnay, S. Inal, A. Salleo, R. M. Owens, M. Berggren, G. G. Malliaras, M. Berggren, R. M. Owens, J. Rivnay, S. Inal, A. Salleo, *Nat. Rev. Mater.* **2018**, *3*, 17086.
[5] K. Melzer, M. Brändlein, B. Popescu, D. Popescu, P. Lugli, G. Scarpa, *Faraday Discuss.* **2014**, *174*, 399.
[6] J. Kofler, K. Schmoltner, E. J. W. List-Kratochvil, *Proc. SPIE*, **2014**, *9185*, 91851U.
[7] C. N. R. Rao, K. Gopalakrishnan, U. Maitra, *ACS Appl. Mater. Interfaces* **2015**, *7*, 7809.
[8] J. Rivnay, S. Inal, A. Salleo, R. M. Owens, M. Berggren, G. G. Malliaras, *Nat. Rev. Mater.* **2018**, *3*, 17086.
[9] L. Kergoat, B. Piro, M. Berggren, G. Horowitz, M. C. Pham, *Anal. Bioanal. Chem.* **2012**, *402*, 1813.
[10] D. Khodagholy, J. Rivnay, M. Sessolo, M. Gurfinkel, P. Leleux, L. H. Jimison, E. Stavrinidou, T. Herve, S. Sanaur, R. M. Owens, G. G. Malliaras, *Nat. Commun.* **2013**, *4*, 2133.
[11] R. A. Picca, K. Manoli, E. Macchia, A. Tricase, C. Di Franco, G. Scamarcio, N. Cioffi, L. Torsi, *Front. Chem.* **2019**, *7*, 667.
[12] K. S. Novoselov, *Science* **2004**, *306*, 666.
[13] C. J. L. de la Rosa, G. Arutchelvan, I. Radu, D. Lin, C. Huyghebaert, M. Heyns, S. De Gendt, *ECS J. Solid State Sci. Technol.* **2016**, *5*, Q3072.
[14] B. Cho, M. G. Hahm, M. Choi, J. Yoon, A. R. Kim, Y. J. Lee, S. G. Park, J. D. Kwon, C. S. Kim, M. Song, Y. Jeong, K. S. Nam, S. Lee, T. J. Yoo, C. G. Kang, B. H. Lee, H. C. Ko, P. M. Ajayan, D. H. Kim, *Sci. Rep.* **2015**, *5*, 8052.
[15] M. Y. Li, S. K. Su, H. P. Wong, L. J. Li, *Nature* **2019**, *567*, 169.

[16] Z. Lin, B. R. Carvalho, E. Kahn, R. Lv, R. Rao, H. Terrones, M. A. Pimenta, M. Terrones, *2D Mater.* **2016**, *3*, 022002.
[17] Z. Hu, Z. Wu, C. Han, J. He, Z. Ni, W. Chen, *Chem. Soc. Rev.* **2018**, *47*, 3100.
[18] S. S. Chee, W. J. Lee, Y. R. Jo, M. K. Cho, D. W. Chun, H. Baik, B. J. Kim, M. H. Yoon, K. Lee, M. H. Ham, *Adv. Funct. Mater.* **2020**, *30*, 1908147.
[19] D. M. Sim, M. Kim, S. Yim, M. J. Choi, J. Choi, S. Yoo, Y. S. Jung, *ACS Nano* **2015**, *9*, 12115.
[20] S. Dalgleish, L. Reissig, Y. Shuku, G. Ligorio, K. Awaga, E. J. W. List-Kratochvil, *Sci. Rep.* **2019**, *9*, 16682.
[21] Y. Huang, E. Sutter, L. M. Wu, H. Xu, L. Bao, H.-J. Gao, X.-J. Zhou, P. Sutter, *ACS Appl. Mater. Interfaces* **2018**, *10*, 23198.
[22] J. Guo, J. Jiang, B. Yang, *Solid State Electron.* **2018**, *150*, 8.
[23] R. A. Picca, K. Manoli, E. Macchia, L. Sarcina, C. Di Franco, N. Cioffi, D. Blasi, R. Österbacka, F. Torricelli, G. Scamarcio, L. Torsi, *Adv. Funct. Mater.* **2020**, *30*, 1904513.
[24] M. Heyl, D. Burmeister, T. Schultz, S. Pallasch, G. Ligorio, N. Koch, E. J. W. List-Kratochvil, *Phys. Status Solidi RRL* **2020**, *14*, 2000408.
[25] S. B. Desai, S. R. Madhvapathy, M. Amani, D. Kiriya, M. Hettick, M. Tosun, Y. Zhou, M. Dubey, J. W. Ager, D. Chrzan, A. Javey, *Adv. Mater.* **2016**, *28*, 4053.
[26] D. Voiry, J. Yang, M. Chhowalla, *Adv. Mater.* **2016**, *28*, 6197.
[27] S. Fathipour, P. Pandey, S. Fullerton-Shirey, A. Seabaugh, *J. Appl. Phys.* **2016**, *120*, 234902.
[28] D. Braga, M. Ha, W. Xie, C. D. Frisbie, *Appl. Phys. Lett.* **2010**, *97*, 193311.
[29] S. Zhang, H. M. Hill, K. Moudgil, C. A. Richter, A. R. Hight Walker, S. Barlow, S. R. Marder, C. A. Hacker, S. J. Pookpanratana, *Adv. Mater.* **2018**, *30*, 1806345.
[30] M. A. Stoeckel, M. Gobbi, T. Leydecker, Y. Wang, E. Eredia, S. Bonacchi, R. Verucchi, M. Timpel, M. V. Nardi, E. Orgiu, P. Samorì, *ACS Nano* **2019**, *13*, 11613.